4th IASPEI / IAEE International Symposium:

Effects of Surface Geology on Seismic Motion

August 23–26, 2011 · University of California Santa Barbara

A NEW STRATEGY FOR DEVELOPING VS30 MAPS

David J. Wald
U.S. Geological Survey
Golden, CO 80401
USA

Leslie McWhirter
Colorado School of Mines
Golden, CO 80401
USA

Eric Thompson
Tufts University
Medford, MA 02155
USA

Amanda S. Hering
Colorado School of Mines
Golden, CO 80401
USA

ABSTRACT

Despite obvious limitations as a proxy for site amplification, the use of time-averaged shear-wave velocity over the top 30 m (Vs_{30}) is useful and widely practiced, most notably through its use as an explanatory variable in ground motion prediction equations (and thus hazard maps and ShakeMaps, among other applications). Local, regional, and global Vs_{30} maps thus have diverse and fundamental uses in earthquake and engineering seismology. As such, we are developing an improved strategy for producing Vs_{30} maps given the common observational constraints available in any region for various spatial scales. We investigate a hierarchical approach to mapping Vs_{30}, where the baseline model is derived from topographic slope because it is available globally, but geological maps and Vs_{30} observations contribute, where available. Using the abundant measured Vs_{30} values in Taiwan as an example, we analyze Vs_{30} versus slope per geologic unit and observe minor trends that indicate potential interaction of geologic and slope terms. We then regress Vs_{30} for the geologic Vs_{30} medians, topographic-slope, and cross-term coefficients for a hybrid model. The residuals of this hybrid model still exhibit a strong spatial correlation structure, so we use the kriging-with-a-trend method (the trend is the hybrid model) to further refine the Vs_{30} map so as to honor the Vs_{30} observations. Unlike the geology or slope models alone, this strategy takes advantage of the predictive capabilities of the two models, yet effectively defaults to ordinary kriging in the vicinity of the observed data, thereby achieving consistency with the observed data.

Keywords: Vs30, topographic slope, geology, kriging, site amplification condition

INTRODUCTION

Recognition of the importance of the ground-motion amplification from regolith has led to the development of systematic approaches to quantifying both amplitude- and frequency-dependent site amplification (e.g., Borcherdt, 1994), as well as schemes for regionally mapping seismic site conditions (e.g., Park and Elrick, 1998; Wills *et al.*, 2000; Holzer *et al.*, 2005). Measuring or mapping Vs_{30} was and is still a standard approach for mapping seismic site conditions. In fact, many U.S. building codes require site characterization explicitly as Vs_{30} (e.g., Dobry *et al.*, 2000; Building Seismic Safety Council, BSSC, 2000). In addition, many of the modern ground-motion prediction equations (e.g., Boore and Atkinson, 2008; Chiou and Youngs, 2008) are explicitly calibrated against seismic-station site conditions described with Vs_{30} values, and these in turn are employed in probabilistic (Kalkan *et al*., 2010) as well as real-time hazard assessments, as in ShakeMap (e.g., Wald *et al*., 1999). The use of Vs_{30} as a proxy for site amplification is widespread and important in a number of hazard and risk-related endeavors.

Yet, there is no question that the use of Vs_{30} as a proxy for site amplification has significant limitations, especially its lack of information pertaining to frequency dependence, and its inability to distinguish between the response of velocity gradients and sharp contrasts for which the Vs_{30} may be similar. Castellaro *et al*. (2008), among others, suggested a litany of other limitations in using Vs_{30} as a proxy for site amplification. Notwithstanding its limitations, which we readily acknowledge, a number of important applications, including hazard and risk maps, and ShakeMaps, will continue the use of Vs_{30} given the current lack of systematically available and readily employable alternatives.

An advantage of the use of Vs_{30} measurements rather than more complex site amplification characterizations (e.g., frequency-dependent empirical measurements, or H/V ratios; Lermo and Chávez-García, 1993)—and perhaps one of the reasons it is so widely in use—is the ability to extrapolate Vs_{30} point observations to maps and thus to apply the very limited existing data to important regional hazard mapping applications. It is exactly this advantage—the ability to map a proxy for site amplification over wide areas—upon which we expand in this study.

We first describe existing Vs_{30} mapping strategies. Two of these approaches, using geology- and topographic-slope-based proxies, are attractive in that both are available in many areas of the world and can thus be applied over wide regions. However, as described next, both have limitations as they are currently employed. As a proposed alternative, in areas where numerous Vs_{30} observations have been made, we can utilize them explicitly, both for improving the geology- and slope-based relationships to Vs_{30}, as well as with geostatistical analyses to incorporate the observations directly (kriging with a trend). We use an example from Taiwan to describe this revised strategy for Vs_{30} mapping. Finally, we generalize this approach, outlining an overall "recipe" for hierarchical Vs_{30} map-making, dependent on the available data sources in a particular region and based on the tools described herein. This new mapping strategy provides motivation for collecting Vs_{30} data at any spatial scale, since any new data can be used explicitly in refining Vs_{30} maps: geostatistically, both local point constraints and regional trend removal can be used to reconcile Vs_{30} data on different spatial scales. In turn, these new data sets and the mapping algorithms described will be built into a refined version of the U.S. Geological Survey's Global Vs_{30} Server (http://earthquake.usgs.gov/vs30/).

EXISTING VS30 MAP STRATEGIES

Several methodologies exist for extending the utility of spatially limited Vs_{30} observations to larger areas. On the largest-scale maps, for instance, for microzonation, densely sampled Vs_{30} measurements can simply be spatially interpolated to cover limited regions rich in data. For example, Hunter *et al.* (2010) developed a Vs_{30} map (NEHRP site classes A through E) for the city of Ottawa, Canada by kriging over 600 Vs_{30} points, extracted from multiple geophysical sampling techniques. Effectively, the abundant data were simply contoured, though where data points were less-densely sampled, consideration of known surficial geological boundaries was used in the final contouring. The resulting Vs_{30} map was used for the Ottawa Urban Earthquake Hazard Mapping program. Rarely are such comprehensive Vs_{30} data sets available. More usually, even in well-studied urban areas with high seismic risks, numbers of Vs_{30} measurements reach only into the hundreds and more often the dozens; most urban areas have few openly available Vs_{30} data sets.

Maps of seismic site conditions on more regional scales are not always available because they require substantial investment in geological and geotechnical data acquisition as well as interpretation. For extending limited observations to smaller-scale maps, several strategies are in use. A standard strategy, referred to here as "geology-based", relies on the premise that mapped near-surface geologic units can be reliable indicators of Vs_{30} values within that unit wherever it has been mapped (e.g., Fumal and Tinsley, 1985; Park and Ellrick, 1998; Wills *et al.*, 2000). Surficial geological units are assigned a constant Vs_{30} value usually based either on the median value of Vs_{30} of all observations inclusive to that unit (e.g., Fumal and Tinsley, 1985; Park and Elrick, 1998; Wills and Silva, 1998; Wills *et al.*, 2000, Wills and Clahan, 2006); or, commonly, they are assigned via expert opinion based on Vs_{30} values indicative of these likely values within the geological units based on representative Vs_{30} values.

The geology-based strategy can provide very useful Vs_{30} maps in some cases (e.g., Wills and Clahan, 2006; Wills and Gutirrez, 2008). Yet, there remains a substantial amount of subjectivity in turning the (often) large number of geological units into the sufficiently few groupings needed for numerically assigning median Vs_{30} values to each; there are insufficient Vs_{30} data to constrain all individual units. Since some or many of the units within the groups have not been sampled by Vs_{30} measurements, the uncertainty of the Vs_{30} values are not accounted for and are, in fact, solely dependent on subjective geological inferences. Furthermore, grouping geological units and assigning a Vs_{30} value to each grouping results in a constant value over large areas of the map (e.g., Fig. 1c, after Lee *et al.*, 2001), even though the Vs_{30} observations show much greater, often systematic, spatial variations within those groups (e.g., compare Fig. 1b and 1c). Worse, in many seismically active regions of the world, information about surficial geology and Vs_{30} either does not exist, varies dramatically in resolution and quality, varies spatially, or is not available in digital form.

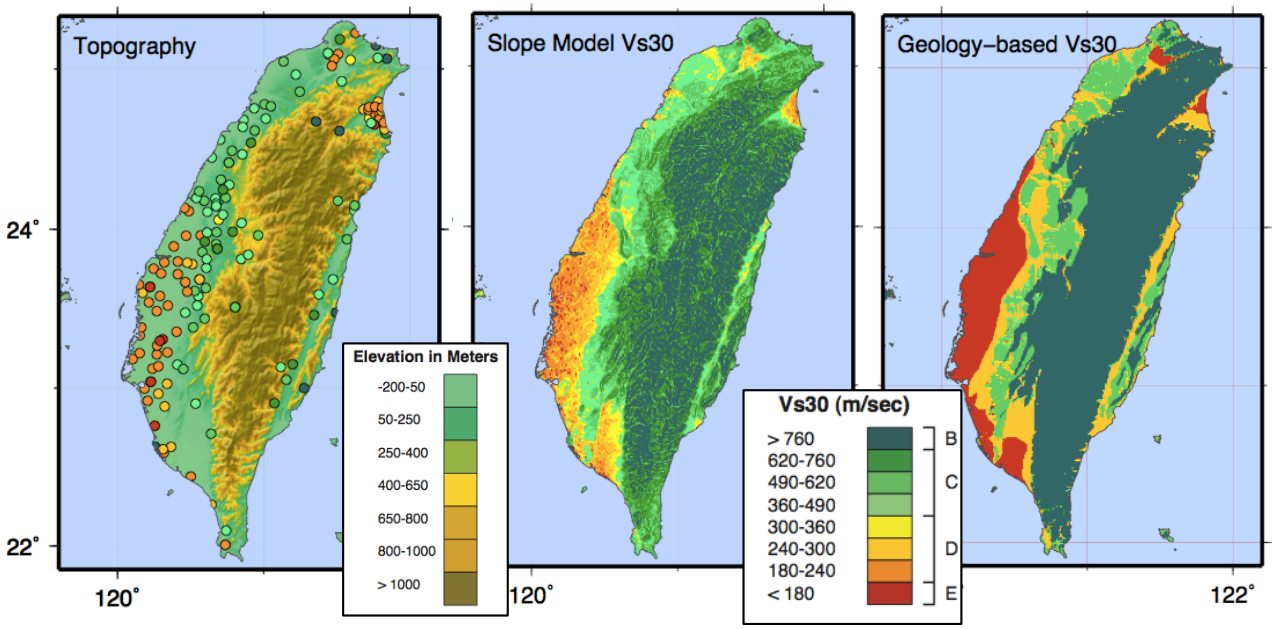

Fig. 1. A) Left: Topographic map of Taiwan at 30 arcsec (~1 km) sampling from STRM data; see legend for elevations. Circles denote Vs_{30} observations (downhole measurements from Lee *et al.*, 2001); color fill is Vs_{30} values (m/sec) as given by NEHRP categories shown in the Vs_{30} legend. B) Middle: Map of Vs_{30} values predicted from the Wald and Allen (2007) model relating topographic-slope to Vs_{30}. C) Right: Geologic-based Vs_{30} map of Lee *et al.* (2001); note Lee *et al.* (2001) use only four discrete categorical geology units.

Topographic elevation data, on the other hand, are available at uniform sampling for the globe (e.g., SRTM data, Farr and Kobrick, 2000). Recognizing the global availability of high-resolution topographic data, Wald and Allen (2007) proposed an alternative approach to systematically estimating and thus mapping Vs_{30} using topographic slope as a predictor of Vs_{30}. By taking the gradient of the topography and choosing ranges of slope that maximize the correlation with shallow shear-velocity observations, they could recover, to first order, many of the spatially varying features of site-condition maps developed for tectonically-active regions like Taiwan and California, as well as for the low-relief, stable-craton regions like the Mississippi Embayment. Notably, the topographic-slope approach also predicted the bulk of the Vs_{30} observations in these regions despite being derived for much wider data sets (Wald and Allen, 2007; Allen and Wald, 2009). Unlike the geology-based approach, the slope-based strategy predicts Vs_{30} values that preserve the character of the observed spatial variations (e.g., compare the Vs_{30} observations in Fig. 1a with Fig. 1b). Subsequent analyses of the topographic-slope proxy for Vs_{30} have shown convincing results (e.g., Wills and Gutierrez, 2008; Thompson *et al.*, 2011) in particular regions, though slope alone was certainly not expected to work well under all geological or geomorphic domains (Wald and Allen, 2007).

Intuitively, topographic variations should be an indicator of near-surface geomorphology and lithology to the first order, with steep mountains indicating rock, nearly flat basins indicating soil, and a transition between the end members on intermediate slopes. Slope of topography, or gradient, should be diagnostic of Vs_{30}, because more competent (high-velocity) materials are more likely to maintain a steep slope whereas deep basin sediments are deposited primarily in environments with very low gradients. Furthermore, particle size or sediment fineness, itself a predictor of lower Vs (e.g., Park and Elrick, 1998), should relate to slope. For example, steep, coarse, mountain-front alluvial fan material typically grades to finer deposits with distance from the mountain front as is deposited at decreasing slopes by less energetic fluvial and ultimately pluvial processes.

When detailed geomorphic, geologic, and geospatial data are systematically available, additional and very logical predictor variables can improve the prediction of measured Vs_{30} values. Matsuoka *et al.* (2005) found impressive correlations with Vs_{30} in Japan among slope, surficial geology, and combinations of geomorphic indicators (for example, man-made fill versus natural fill, distance to mountain front, depositional environment, and elevation). However, outside of Japan, such detailed geomorphic indicators are not widely mapped and are thus not digitally available.

After recognizing the correlation of slope with Vs_{30} within particular quaternary soils units, Wills and Gutierrez (2008) suggested employing slope as a corrective factor over uniform Vs_{30} assignments within basin geological units. This combination of geology and slope was investigated but was not ultimately employed in the map made available for distribution from their study; their revised map employed refined geologic divisions but not the Vs_{30} gradients within those units that slope would suggest.

Yong *et al.* (2008) employed semi-automated digital imaging analyses of Advanced Space-borne Thermal Emission and Reflection Radiometer (ASTER) satellite imagery, combined with topography based on the same SRTM (30 arc-second sampling) data used by Wald and Allen (2007), to break up topographic variations (e.g., slope, convexity, and roughness) into assignments to terrain units (e.g., mountain, piedmont, and basin). These terrain units were then assigned Vs_{30} ranges by average observations within those units. However, many of the units were poorly sampled by Vs_{30} data, and the lack of diverse lower-velocity units limit resolution at low Vs_{30} (high amplification). As their approach relied only on remotely-sensed data, it too can potentially be applied globally. However, it is unclear how the terrain unit assignments are independent of the slope and geologic-based predictor variables used in earlier studies.

One limiting aspect of all these state-of-the-art strategies for generating estimated Vs_{30} maps, whether from geologic (e.g., Wills *et al.*, 2000; Wills and Clahan, 2006) or topographic base maps (e.g., Wald and Allen, 2007; Allen and Wald, 2009), or terrain (Matsuoka *et al*., 2005; Yong *et al*., 2008) predictors is that, while initially derived from or constrained by observed Vs_{30} values, these approaches fail to directly incorporate the Vs_{30} measurements used back into the map that has been created. Likewise, there are no strategies in place for accommodating clear regional trends that obviously deviate from *a priori* slope or geology trend models, especially when significant, new Vs_{30} data become available. For example, Fig. 2 shows a comparison of logarithmic trends of topographic slope versus measured Vs_{30} for Taiwan (black) and for the Salt Lake City, Utah region (red). Regional trends in the relationship between Vs_{30} and slope may be significant, and perhaps related to the nature of the geologic units, and controlled by variations in depositional and active tectonic environments. Moving forward, we have developed a strategy to not only directly incorporate all available Vs_{30} into the mapping process, but to also let these data inform the recalibration, removing any regional trends in Vs_{30} versus slope as well as geology.

A REVISED VS30 MAPPING STRATEGY

For combining Vs_{30} data directly into a joint model of Vs_{30} (i.e., topographic slope-based or geology-based) we will employ the geostatistical strategy of kriging. What makes kriging special is that it accounts for the spatial dependence among observations. Kriging allows us to estimate Vs_{30} at unsampled locations from the observed values; kriging itself is a generalized least-squares regression algorithm. Any sufficiently well-sampled Vs_{30} data can also be used to refine our *a-priori* predictive models, so rather than ordinary kriging, we can employ kriging with a trend (KT; for more background see, for example, Thompson *et al.*, 2010). Simple kriging (SK) assumes that the trend is known and constant, ordinary kriging (OK) assumes it is unknown but still constant, and kriging with a trend (KT), also known as "universal kriging," allows the trend to fluctuate in space (Goovaerts, 1999). The geostatistical literature often employs many different terms for what are rather similar techniques. Universal kriging, kriging with external drift, and regression-kriging are basically the same.

The two potential trends we explore, topographic slope and geology, will be modified by inverting for the best-fit coefficients for slope and mean Vs_{30} per geologic unit. Here we take advantage of the notion that the drift and residuals can be estimated separately and then summed (e.g., Thompson *et al.*, 2010). These revised trends will be removed from the data, and since the residuals of this hybrid model exhibit a strong spatial correlation structure, we will use the kriging with a trend method (the trend is the hybrid model) to further refine the Vs_{30} model-based map with the observed Vs_{30} values. In a sense, we are modeling both the deterministic (trend) and stochastic (variability) components of spatial Vs_{30} variations separately. Unlike the geology or slope models alone, this strategy takes advantage of the predictive capabilities of the both the geology and slope models, and potentially their interaction, yet effectively defaults to ordinary kriging in the vicinity of the observed data, thereby achieving consistency with the observed data.

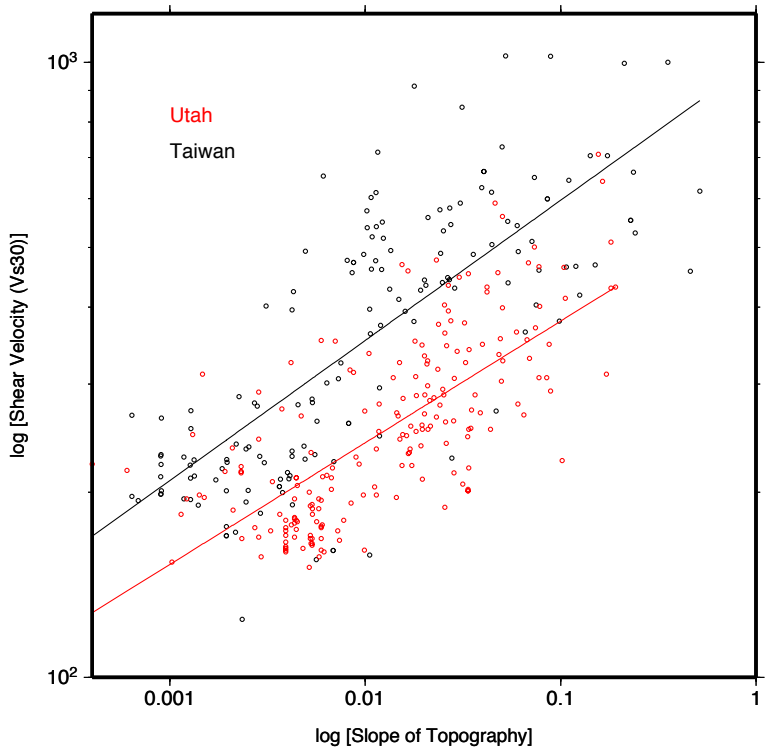

Fig. 2. Comparison of measured Vs_{30} (m/sec) versus topographic slope (m/m) for Taiwan (black) and the Salt Lake City, Utah region (red). The lines represent least-squares fits separately for the Taiwan and Salt Lake City data. The linear fits have similar slopes, but the fit for the Taiwan data is vertically shifted from the fit for the Salt Lake City data. This consistent difference between predicted Vs30 values for Taiwan and Salt Lake City may be explained by the varied depositional and active orogenic environments.

MODELING AND RESULTS

Determining the optimal coefficients for slope, mean geological Vs_{30} values, and any interactions (cross-terms) can be solved using ordinary least squares (OLS) or, more optimally, using Generalized Least Squares (GLS). Ideally, any remaining correlation in the covariance function of the residuals from OLS would be used iteratively to obtain the GLS coefficients, but such a strategy is unlikely to be warranted given the limited amount and quality of the typical Vs_{30} data set. GLS could be explored with a more comprehensive Vs_{30} data set than what is available for Taiwan (perhaps the Vs_{30} data for the city of Ottawa, Canada; e.g., Hunter *et al.*, 2010).

The primary variable of interest is Vs_{30}, which we assume to be log-normally distributed. If we let $y = \log_{10}(Vs_{30})$, for example, given four geologic units, we can express the OLS model as:

$$y = \beta_0 + \beta_1 x_1 + \beta_2 x_2 + \beta_3 x_3 + \beta_4 x_4 + \beta_5 x_1 x_4 + \beta_6 x_2 x_4 + \beta_7 x_3 x_4 + e \quad (1)$$

Here, x_1, x_2, and x_3 are indicator variables for the geologic units, x_4 denotes the topographic slope, β_1, β_2, and β_3 are factors adjusting the intercept of the baseline geology units, and β_5, β_6, and β_7 are adjustments to the slope within the same units, β_0 represents the combined slope and geology intercept, and e is a residual term. In general, any interaction terms, say β_7, could be insignificant if the relationships between slope and observed Vs_{30} for units $x_3 x_4$ are similar, and could be dropped. Likewise, fewer or more than four geological units could be easily represented and corresponding coefficients could be determined.

If it is deemed that interaction terms are unnecessary, or the coefficients cannot be constrained, we drop those terms:

$$y = \beta_0 + \beta_1 x_1 + \beta_2 x_2 + \beta_3 x_3 + \beta_4 x_4 + e \quad (2)$$

Conversely, where individual geological classes are not well sampled, only modifications to the general slope terms are afforded, and the resulting map will default to the slope model, modified with the model residuals (Vs_{30} data) as described below. Likewise, in regions were geologic maps are either inadequate or are not digitally available, we let $x_1 = x_2 = x_3 = 0$, so any local Vs_{30} data can be used for solving for only the baseline and slope terms of the topographic-slope model:

$$y = \beta_0 + \beta_4 x_4 + e \tag{3}$$

Any remaining spatially-correlated residuals in the data from that trend can be kriged as described below. First, determining whether or not cross-terms (allowing variations of slope coefficients within each geologic unit) are needed must be explored by examining whether or not slope trends can be found to exist (and differ) among and within individual geological units. If cross terms are unneeded, a single slope coefficient is sufficient among the geological categories explored, or that there are insufficient data to justify variable slopes per unit.

Regional variations in the relationship between slope and Vs30 were noted by Wald and Allen (2007); they found obvious differences in slope-Vs_{30} correlations between regions with active tectonics versus stable shields. Allen and Wald (2007) also noticed more subtle variations within tectonically active areas, though the limited Vs_{30} data limited resolution of these differences in all but the best data sets. Given the likely dependence of slope versus Vs_{30} on a variety of geologic sources and processes, perhaps it is not surprising to find such differences, yet lacking an understanding of the dominant physical mechanisms controlling these relationships, we should use care when interpreting them. However, in Fig. 2, there is clearly a distinguishable offset in the slope-Vs_{30} relationship between Taiwan and Utah; such differences require different trends among different regions. Next, we explore if such trend differences are significant and distinguishable among different geologic units within our region of interest.

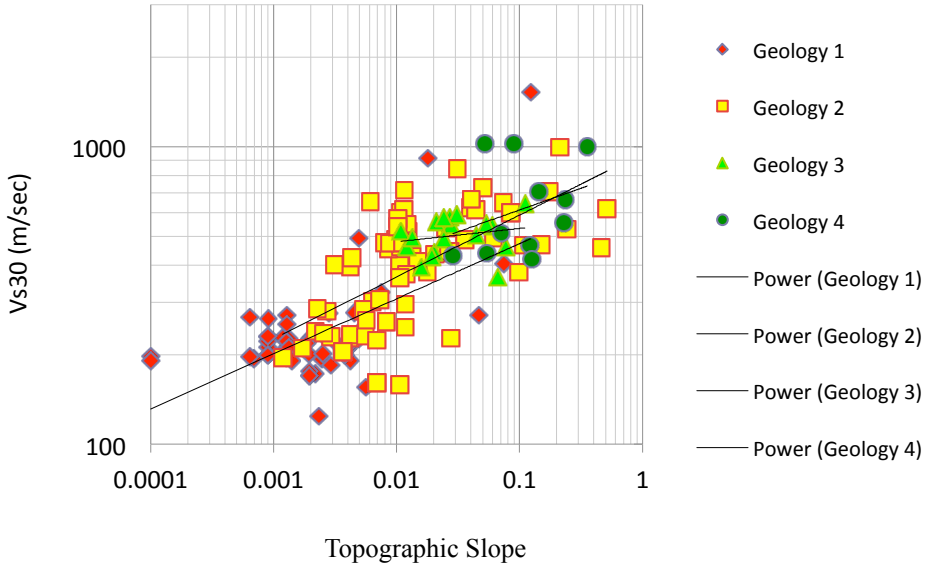

Fig. 3. Comparison of slope (m/m) and Vs_{30} for Taiwan separated by geologic units. Color-coding for geological units is similar to those shown in Fig. 1b. Lines are individual linear regressions for the Vs_{30} for each unit.

In Fig. 3, we separate the Taiwan Vs_{30} observations versus topographic slope by geologic unit to make exploratory scatter plots to see if slope trends vary among the units. Separate Vs_{30} versus slope trends among the geologic units would justify cross-terms, allowing the mean geology and slope within a unit to behave independently of other units. We can then jointly regress Vs_{30} from the geologic classifications and the topographic-slope to derive coefficients for Vs_{30} versus slope, the median geologic Vs_{30} value, and offset as well as cross terms. As seen in Fig. 3, some units have data with limited ranges of slope making comparison risky, yet the similarity in trends does not strongly support the use of cross terms for a differing slope term within each geologic unit in this case. Thus, in the current analysis, we limit our regression to equation (2).

Next, we need to process Vs_{30} data points, gridded topographic data, and polygonal, categorical geological data. In practice, the grid calculations and map-making are done using GMT (Wessel and Smith, 1995), and our kriging and regressions are done in R (R Development Core Team, 2010). A flowchart of the procedure is provided in Fig. 4. In GMT, we compute the maximum slope from the topography (Fig. 1a) as outlined by Wald and Allen (2007). The geological units (Fig. 1c), initially GIS shapefiles, are then

sampled at the same 30 arc-second sampling grid sampling as the topographic slope. The values of slope and geology category are determined at each Vs_{30} observation location. Then using R, we regress the equation (2) using ordinary least squares to determine the coefficients, which are passed back to GMT.

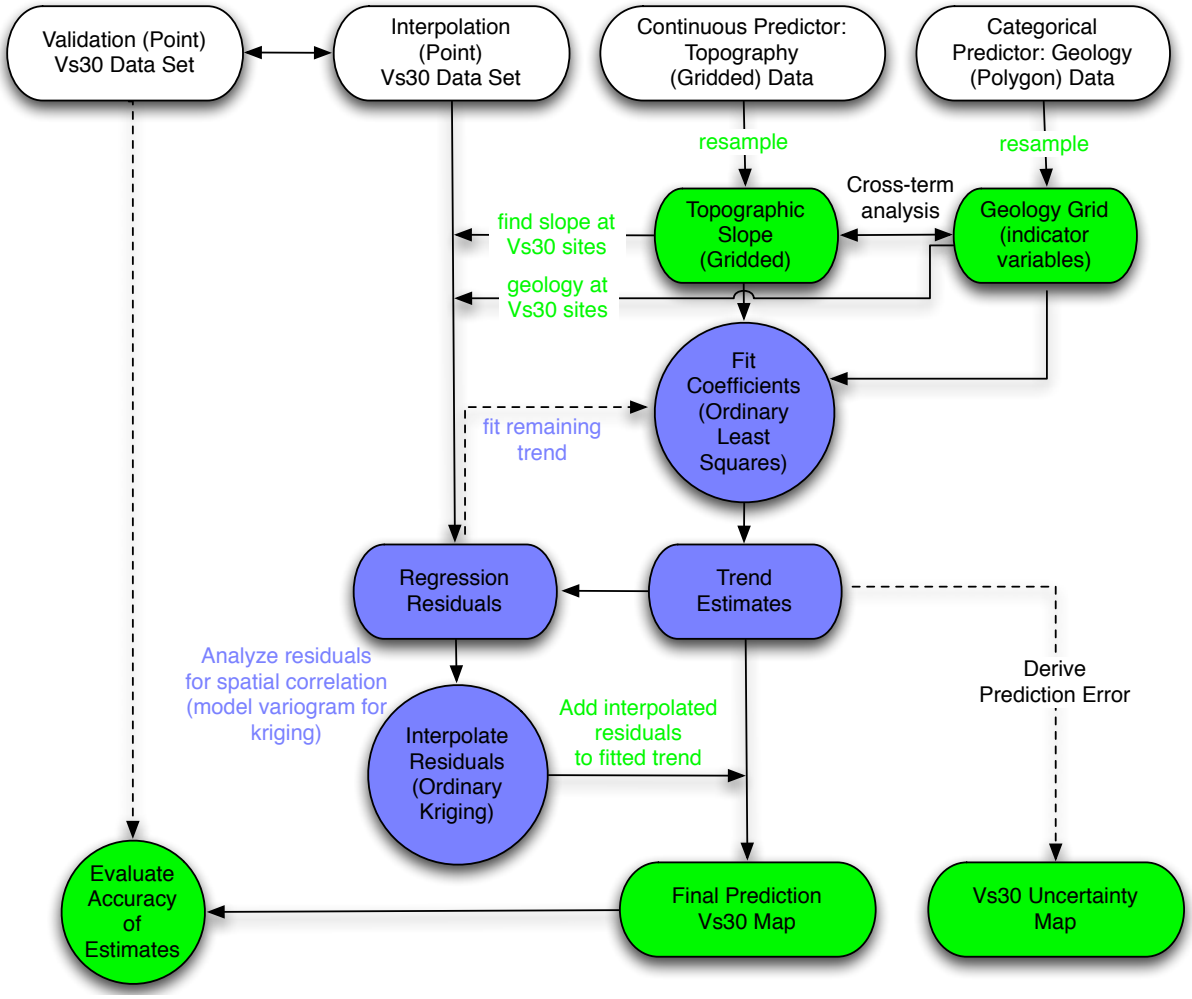

Fig. 4. Flow chart for data processing, data analysis, regression modeling, and kriging. GMT processes are shown in green; R functions in blue; white ovals are input data sets. Validation, refitting, and prediction error calculations (dashed lines) have not yet been attempted. See text for details.

The forward calculation, estimating Vs_{30} at all grid points, is done efficiently with GMT's grid math processing and the results are mapped in Fig. 5b. Next, residuals of the Vs_{30} data from the forward model are determined at each observation point. Back in R (Fig. 3), kriging preprocessing involves generating and fitting a variogram (usually an exponential function) and determination of appropriate sill, nugget, and range values (Fig. 6). The residuals are then kriged using these data-specific spatial correlation values, and the results are resampled on the same uniform grid, which can be mapped back in GMT (Fig. 5c). Finally, the gridded, kriged residuals are summed directly with the joint slope and geologic trend model to form the final Vs_{30} map (Fig. 5d).

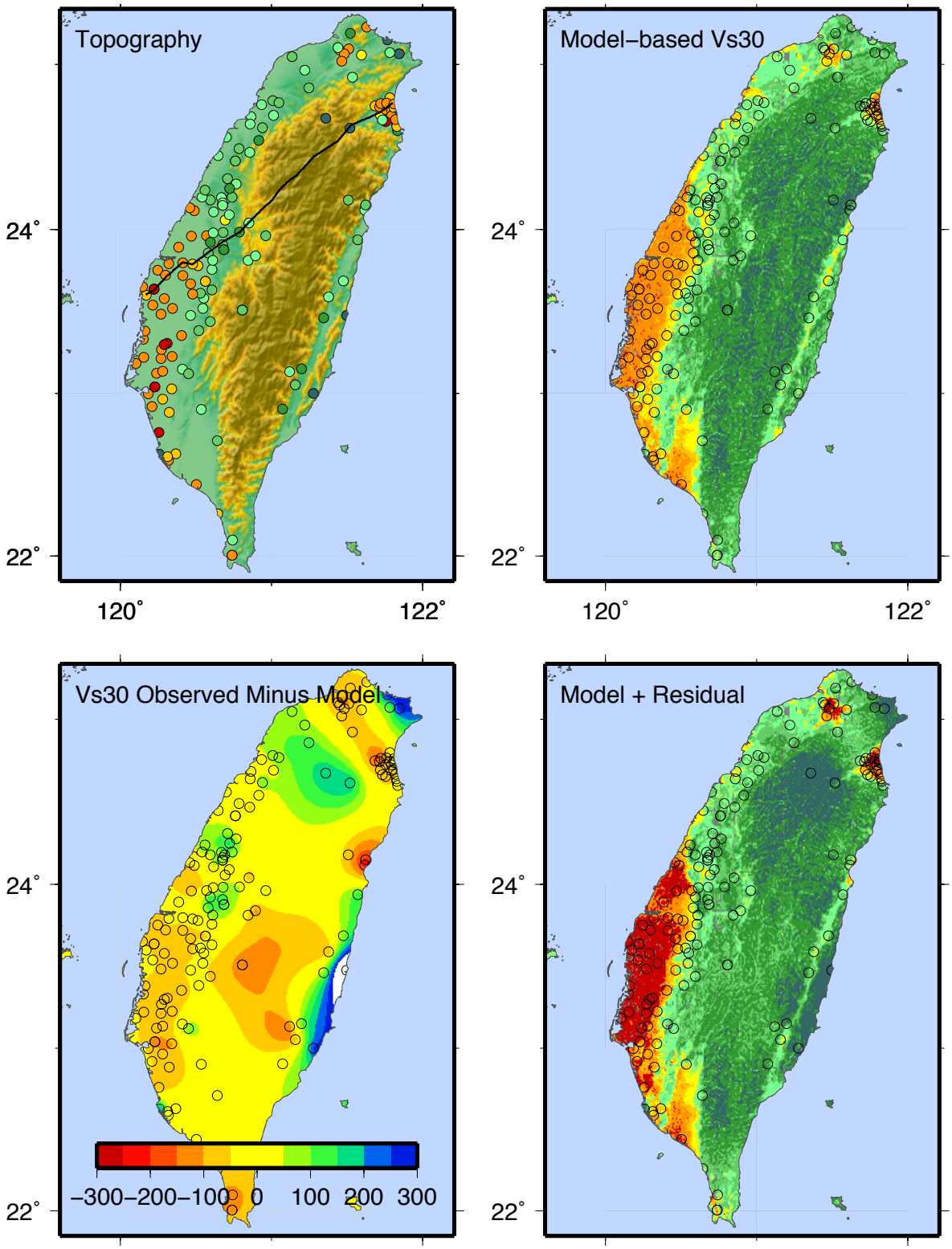

Fig. 5. a) Upper left: Topographic map and Vs_{30} data for Taiwan; see Fig. 1 for details and legend. Black line shows the profile of observations shown in Fig. 7; b) Upper right: map of Vs_{30} trend model estimated with the combined slope and geology-based relations derived by regression. c) Lower left: kriged residuals of Vs_{30} observations (a) minus the trend model (b); see legend for residual values (m/sec). d) Lower right: Final map generated by adding the kriged residuals (c) back onto the slope-based model (b)

From analysis of Fig. 5, we can see the desired contributions of the individual model components: the eastward gradient of Vs_{30} from along west coast of Taiwan in the combined trend model (Fig. 5b), and within a single geologic unit (see Fig. 1c), indicates the slope-based contribution; the plume-shaped, southernmost NEHRP E-category geologic unit (Fig. 1c; near 120.3E, 22.3N) in the combined trend model indicates some degree of geologic control; and, the modification of the trend model by the data as seen in Fig. 4d, clearly indicates the role of individual Vs_{30} data on the final model, for example, at and around the slowest Vs_{30} sites in valleys and along the west coast, or in the lowering of final Vs_{30} values in the mountains in the north-central portion of the island.

The final combined trend model Fig. 5b more closely resembles the original (Fig.1b; Wald and Allen (2007) slope-based model than the geologic-based model (Fig. 1c), though the slope model overestimated Vs_{30} at some northern basin sites. In case of Taiwan, the slope-model dominance is attributed to the favorable initial agreement of the Wald and Allen model with the observed Vs_{30} and the clear trends of Vs_{30} within the separate, homogenous geologic units. It remains to be seen if this slope-model dominance will be the norm in other tectonic or geomorphic environments. Clearly, however, the final Vs_{30} map (Fig. 5d) is an improvement over the Wald and Allen (2007) slope-based model in that it more closely matches observations at individual Vs_{30} sites (Fig. 5a). A profile across Taiwan (black line in Fig. 5a) is provided in Fig. 7, comparing Vs_{30} values along section for the trend model (dashed line) and for the final model with the kriged residuals added back in (Fig. 5d).

DISCUSSION

Although the procedure outlined here has only been applied, in this case, to one region, in essence we are proposing a simple "recipe" for developing Vs_{30} maps which should be generally applicable to any region of the world. In the absence of any Vs_{30} data, or geologic maps, the default becomes a slope-based Vs_{30} map using predetermined Vs_{30}–slope correlations determined for a comparable tectonic environment elsewhere. With the addition of sufficient Vs_{30} data (say, a few dozen values), the slope-Vs_{30} correlation can be refined, improving on a default trend, regressing for only the slope (of topographic slope versus Vs_{30}) and intercept coefficients (equation 2). If geological maps are available, determine if cross-terms are needed, and adjust the use of equation (1) adding cross-terms accordingly. The complete strategy for regression-kriging is then performed as described above, shown graphically in the flowchart in Figure 5, is outlined here:

1) Assemble data sets:
    a. Point Vs_{30} data and uncertainties (down-hole, SASW, ReMi, CPT, etc.)
    b. Assess the quality of the point data, assigning weights to reflect the quality of the measurements if necessary.
    c. Digital topography: resolution 30 or 9 arc-second sampling (1 km or 250 m, respectively)
    d. Digital geology maps (or, potentially, other Vs_{30} -proxy maps); convert polygons to grids
2) Data preprocessing:
    a. Topography:
        i. Compute maximum slope values on grid.
        ii. Sample slope at Vs_{30} observation points.
    b. Geology-based Vs_{30} assignments:
        i. Assign categorical (ordinal) values to geology map units.
        ii. Sample geology units at Vs_{30} data points.
3) Solve for combined slope and geology trend model coefficients. Generate forward model.
4) Compute residuals from the observed Vs_{30} values minus the trend model.
5) Analyze Vs_{30} residuals (variogram estimation; determine nugget, sill, and range).
6) Krige Vs_{30} residuals and generate a grid of kriged residuals.
7) Add gridded kriged Vs_{30} residuals back to trend model estimates.
8) Uncertainty analyses: compute cross-validation of data, map uncertainties.

Ongoing improvements in developing an optimal strategy for Vs_{30} map development, include: i) the use of higher-resolution topography (9 rather than 30 arc-second), ii) Employing sufficiency criteria (p-value) for employing topographic slope and geology cross terms (equation 1), and iii) determination of estimated Vs_{30} uncertainties. Allen and Wald (2009) and Wills and Gutirrez (2008) have identified some limitations to higher resolution data, yet we anticipate that switching to 9 arc-second sampling (250-m spacing) topographic data and re-deriving slope coefficients will be beneficial.

A final consideration is refining the Perl, R, and GMT scripts employed for semi-automating the production of Vs_{30} maps in other regions. Manual intervention will still be required for inspecting the variogram model (autocovariance function) needed for kriging

residuals from the trend model. More significant work will be involved for areas in aggregating geological units appropriately and commensurate with the Vs_{30} data available to constrain their averages. A fundamental limitation of the geologic-based approach is the trade-off between improved resolution and finer spatial variations offered by allowing more numerous geologic categories versus the need to sample each with sufficient Vs_{30} observations to constrain its median value.

The next task will be applying our strategy to Vs_{30} data from glaciated terrains in New England and the upper Midwest (not tested by Wald and Allen, 2007, using topographic slope alone), and then apply the "recipe" described above to develop a more refined Vs_{30} map of the United States. In turn, that final product will replace the Vs_{30} map now served by the USGS by their Global Vs30 Server (http://earthquake.usgs.gov/vs30/).

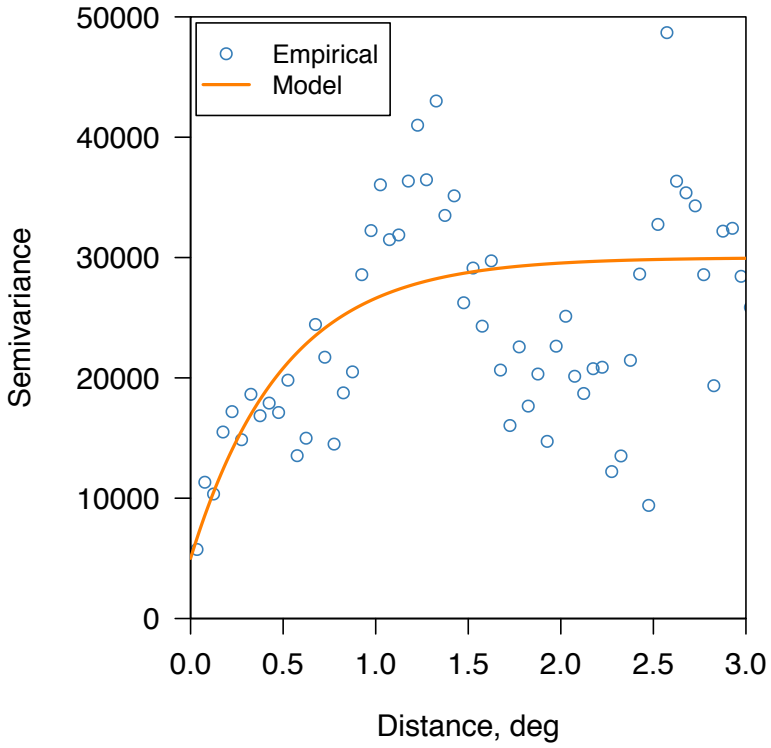

Fig. 6. Spatial correlation variogram for Vs_{30} residuals from the combined model (Fig. 5b). Kriged residuals (5b) employ a 5000 nugget, 25000 sill, and range (cutoff distance) of 0.5 degrees.

CONCLUSIONS

One limiting aspect of current state-of-the-art strategies for generating estimated Vs_{30} maps, whether from geologic, topographic, or remotely sensed base maps, is that although derived from or aimed to be consistent with observed Vs_{30} values, these approaches fail to directly incorporate the Vs_{30} observations back into the map that has been created. Likewise, there are no strategies in place for accommodating significant new Vs_{30} data as they become available or where regional trends obviously deviate from the default trend models.

The strategy described herein uses a hierarchical approach to mapping Vs_{30}, taking full advantage of these most commonly available data sources: topographic slope, surficial geological maps, and Vs_{30} measurements. The baseline model is derived from topographic slope because it is available globally, but geological maps and Vs_{30} observations contribute where data are available. We analyze Vs_{30} versus slope per geologic unit and observe minor trends that indicate some interaction of geologic and slope domains, but in the case of Taiwan, not enough to warrant separate regression terms. We then regress Vs30 for the geologic Vs_{30} medians and regional topographic slope-Vs_{30} coefficients for a hybrid topographic-slope/geologic model. The residuals of this hybrid model still exhibit a strong spatial-correlation structure, so we use the kriging-with-a-trend method (the trend is the hybrid model) to insure we fit all Vs_{30} observations at those sites. Unlike the geology or slope models alone, this strategy takes advantage of the predictive capabilities of the

two models, yet effectively defaults to ordinary kriging in the vicinity of the observed data, thereby achieving consistency with the observed data.

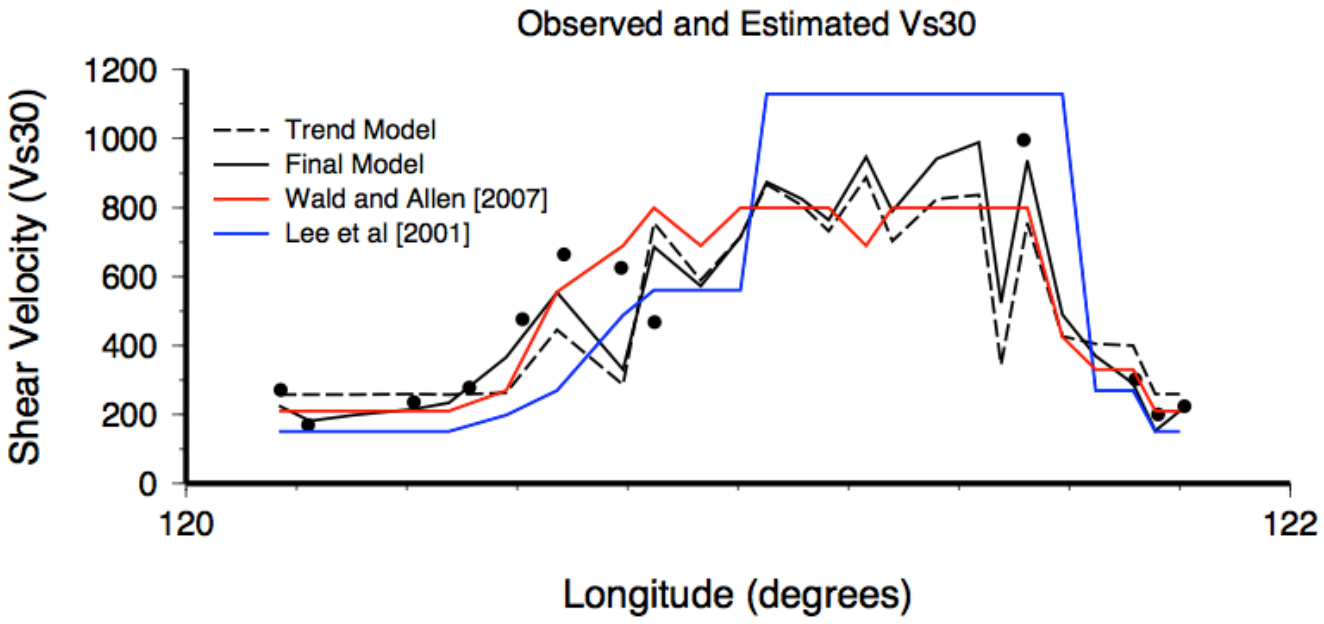

Fig. 7. SW-NE profile (see track line on Fig. 5a) showing Vs_{30} data (circles), and sampling the trend model (dashed, Fig. 5b) and final kriged model (solid line, Fig. 5d). Wald and Allen's (2007) topographic slope-based model (red line) and Lee et al's geology-based model (blue line) are also shown for comparison

ACKNOWLEDGEMENTS

Internal USGS reviews by Bruce Worden and Anna Olsen are greatly appreciated; Bruce also provided needed guidance on GMT's grdmath computations.

REFERENCES

Allen, T. I. and D. J. Wald [2009]. On the Use of High-Resolution Topographic Data as a Proxy for Seismic Site Conditions (VS_{30}), *Bull. Seism. Soc. Am*., **99**, No. 2A, pp. 935–943.

Allen, T. I. and D. J. Wald [2007]. Topographic Slope as a Proxy for Seismic Site Conditions (*VS*30) and Amplification around the Globe, *U.S.G.S. Open File Report* 2007-1357, 69 pp.

Boore, D. M., and G. M. Atkinson [2008]. Ground-Motion Prediction Equations for the Average Horizontal Component of PGA, PGV, and 5%-Damped PSA at Spectral Periods between 0.01 s and 10.0 s. *Earthquake Spectra*, 24(1), 99-138.

Boore, D.M., Asten, M.W. [2008]. Comparisons of shear-wave slowness in the Santa Clara Valley, California, from blind interpretations of data from a comprehensive set of invasive and non-invasive methods using active- and passive-sources. *Bull. Seism. Soc. Am*., **98**, 1982–2003.

Borcherdt, R. D. [1994]. Estimates of site-dependent response spectra for design (methodology and justification), *Earthquake Spectra,* **10**, 617-653.

Building Seismic Safety Council (BSSC) [2000]. *National Earthquake Hazards Reduction Program (NEHRP) Part 1: Recommended provisions for seismic regulations for new buildings and other structures*, Federal Emergency Management Agency.

Castellaro, S., F. Mulargia, P. Rossi [2008]. Vs30: Proxy for site amplification?, *Seism. Res. Lett.*, **79**, 540-544.

Chiou, B. S.-J., and R. R. Youngs [2008]. An NGA Model of the Average Horizontal Component of Peak Ground Motion and Response Spectra. Earthquake Spectra, 24(1), 173-215.

Dobry, R., R. D. Borcherdt, C. B. Crouse, I. M. Idriss, W. B. Joyner, G. R. Martin, M. Power, E. Rinne, and R. B. Seed [2000]. New site coefficients and site classification system used in recent Building Seismic Code provisions, *Earthquake Spectra,* **16**, 41-67.

Farr, T. G., and M. Kobrick [2000]. Shuttle Radar Topography Mission produces a wealth of data, *EOS Trans.,* **81**, 583-585.

FEMA [1994]. *NEHRP recommended provisions for the development of seismic regulations for new buildings*, FEMA.

Fumal, T. E., and J. C. Tinsley [1985]. Mapping shear-wave velocities of near-surface geologic materials, *Evaluating Earthquake Hazards in the Los Angeles Region-An Earth-Science Perspective* 1360, 101-126.

Goovaerts, P. [1999]. Geostatistics in soil science: state-of-the-art and perspectives, *Geoderma*, **89**, 1–45.

Holzer, T. L., A. C. Padovani, M. J. Bennett, T. E. Noce, and J. C. Tinsley [2005]. Mapping Vs30 site classes, *Earthquake Spectra*, **21**, 353-370.

Hunter, J A; Crow, H L; Brooks, G R; Pyne, M; Motazedian, D; Lamontagne, M; Pugin, A J -M; Pullan, S E; Cartwright, T; Douma, M; Burns, R A; Good, R L; Kaheshi-Banab, K; Caron, R; Kolaj, M; Folahan, I; Dixon, L; Dion, K; Duxbury, A; Landriault, A; Ter-Emmanuil, V; Jones, A; Plastow, G; Muir, D. [2010]. Seismic site classification and site period mapping in the Ottawa area using geophysical methods, *Geological Survey of Canada Open File* 6273, 80 pages.

Kalkan, E., C. J. Wills, and D. M. Branum [2010]. Seismic Hazard Mapping of California Considering Site Effects, *Earthquake Spectra*, **26**, No. 4, pages 1039–1055.

Lee, C.-T., C.-T. Cheng, C.-W. Liao, and Y.-B. Tsai [2001]. Site classification of Taiwan free-field strong-motion stations, *Bull. Seism. Soc. Am.,* **91**, 1283-1297.

Lermo, J., and F. J. Chávez-García [1993]. Site effect evaluation using spectral ratios with only one station, *Bull. Seism. Soc. Am*., **83**, no. 5, 1574–1594.

Matsuoka, M., K. Wakamatsu, K. Fujimoto, and S. Midorikawa [2005]. Nationwide site amplification zoning using GIS-based Japan engineering geomorphologic classification map, *Proc. 9th Inter. Conf. on Struct. Safety and Reliability*, 239-246.

Park, S., and S. Elrick [1998]. Predictions of shear-wave velocities in southern California using surface geology, *Bull. Seism. Soc. Am.,* **88**, 677-685.

R Development Core Team [2010]. R: A Language and Environment for Statistical Computing, R Foundation for Statistical Computing, Vienna, Austria.

Thompson, E. M., L. G. Baise, R. E. Kayen, E.C. Morgan, and J. Kaklamanos [2011]. Multiscale Site-Response Mapping: A Case Study of Parkfield, California, *Bull. Seism. Soc. Am*., **101**, 1081–1100.

Thompson, E. M., L. G. Baise, R. E. Kayen, Y. Tanaka, and H. Tanaka [2010]. A geostatistical approach to mapping site response spectral amplifications, *Eng. Geol*., **114**, no. 3–4, 330–342.

USGS Global Vs30 Server [2011]. 30-arc-sec resolution global slope-based Vs30 proxy maps. http://earthquake. usgs.gov/vs30/.

Wald, D. J., P. S. Earle, and V. Quitoriano [2004]. Topographic Slope as a Proxy for Seismic Site Correction and Amplification, *EOS. Trans*. AGU, **85**(47), F1424.

Wald, D. J., and T. I. Allen [2007]. Topographic slope as a proxy for seismic site conditions and amplification, *Bull. Seism. Soc. Am.*, **97**, No. 5, 1379-1395.

Wald, D. J., V. Quitoriano, T.H. Heaton, H. Kanamori, C.W. Scrivner and C.B. Worden [1999]. TriNet "ShakeMaps": Rapid generation of peak ground motion and intensity maps for earthquakes in southern California, *Earthquake Spectra*, 15, 537-555.

Wessel, P., and W. H. F. Smith [1995]. New Version of the Generic Mapping Tools Released, *EOS Trans. AGU, 76*, 329.

Wills, C. J. and C. Gutierrez [2008]. Investigation of geographic rules for improving site-conditions mapping, *Calif. Geo. Sur. Final Tech. Rept.*, 20 pp. (Award No. 07HQGR0061).

Wills, C. J., and K. B. Clahan [2006]. Developing a map of geologically defined site-condition categories for California, *Bull. Seism. Soc. Am.*, **96**, 1483–1501.

Wills, C. J., M. Petersen, W. A. Bryant, M. Reichle, G. J. Saucedo, S. Tan, G. Taylor, and J. Treiman [2000]. A site-conditions map for California based on geology and shear-wave velocity, *Bull. Seism. Soc. Am.*, **90**, S187–S208.

Wills, C. J., and W. Silva [1998]. Shear-wave velocity characteristics of geologic units in California, *Earthquake Spectra,* **14**, 533-556.

Yong, A., Hough, S.E., Abrams, M.J., Cox, H.M., Wills, C.J., Simila, G.W. [2008]. Site characterization using integrated imaging analysis methods on satellite data of the Islamabad, Pakistan, Region, *Bull. Seism. Soc. Am.* **98**, 2679–2693.